RAPID COMMUNICATION

Minority carrier barrier heterojunctions for improved thermoelectric efficiency

Peter G. Burke[a,*], Benjamin M. Curtin[b], John E. Bowers[a,b], Arthur C. Gossard[a]

[a]*Materials Department, University of California, Santa Barbara, United States*
[b]*Electrical and Computer Engineering Department, University of California, Santa Barbara, United States*

Abstract
We propose and demonstrate the beneficial use of minority carrier blocking layers to lessen bipolar conduction at elevated temperatures and increase the Seebeck coefficient in a thermoelectric material. Bipolar conduction, caused by thermally activated intrinsic carriers in semiconductors, causes a detrimental "roll-over" in the Seebeck coefficient and increase in thermal conductivity, measured as a function of temperature. We propose that these negative effects can be lessened or delayed in a small band gap host matrix by incorporating wider band gap semiconductor layers to impede the thermal diffusion of minority carriers over majority carriers. To prove this concept, a composite material grown by molecular beam epitaxy of p-type InAs layers and electron blocking p-type AlSb layers were grown and measured. We show improved thermoelectric properties over just p-type InAs in measurements from 110 K to 600 K.
© 2015 Elsevier Ltd. All rights reserved.

Introduction

The most common contribution to the inefficient use of energy is generation of waste heat [1]. Waste heat is energy that escapes from a system without contributing to the work done. A device capable of capturing that waste heat and turning it back into electricity would inherently increase the efficiency of the system and lower net power consumption. Often the

environment for the most effective heat capture demands that the unit be small, clean, and reliable. It is here, in the niche of energy harvesting, where thermoelectric materials can be of great use [2]. The thermoelectric efficiency of a material is often ranked by the thermoelectric figure of merit, zT, consisting of the Seebeck coefficient, S, electrical conductivity, σ, and thermal conductivity, κ, by $zT = S^2\sigma T/\kappa$. Therefore, the thermoelectric efficiency of a material is improved by increasing its Seebeck coefficient and electrical conductivity and by decreasing its thermal conductivity. However, these parameters are often directly related to each other. Generally for a semiconductor, as the carrier concentration is increased, the

*Corresponding author.
E-mail address: pgb204@gmail.com (P.G. Burke).

electrical conductivity increases but unfortunately, the Seebeck coefficient decreases and the thermal conductivity increases as well. In addition, these parameters are temperature dependent. For most semiconductors, the Seebeck coefficient increases with temperature until it reaches a maximum and begins to decrease. The Seebeck coefficient can even change sign at very high temperature. The reduction in Seebeck coefficient is caused by the thermal activation of intrinsic carriers. When there is mixed n-type and p-type conduction, i. e. bipolar conduction, the negative and positive Seebeck coefficients of each, respectively, cancel each other out. Essentially, both negative charges and positive charges are present within the same material and diffuse along the thermal gradient. In this case, there is no net charge transfer and the Seebeck coefficient is zero.

Conventionally, the temperature at which thermally excited minority carriers cause a decrease in Seebeck coefficient can be raised by using a material with a wider band gap, or by increasing the extrinsic doping [3,4]. In this work, we predict and demonstrate increasing the Seebeck coefficient at higher temperature by utilizing minority carrier blocking layers. By impeding the thermal diffusion of minority carriers, we push the scenario closer to the optimum single-carrier Seebeck coefficient and improve the thermoelectric efficiency. The concept of minority carrier blocking layers is implemented here with wide band gap AlSb layers on narrow band gap InAs layers, grown by molecular beam epitaxy (MBE), but is generally applicable to any combination of semiconductors where the heterojunction can block the flow of the minority carriers but not block the flow of majority carriers.

For example, the concept of confining or blocking charge carriers has been used extensively in semiconductor research before, indeed it is the basis for many optical devices such as solid-state lasers, LEDs, and detectors. Electron- and hole-blocking layers have been used for PbIbN [5,6] and nBn [7] infrared detectors to reduce dark current as compared to conventional PIN detectors. This results in an increase in detectivity and higher operating temperatures.

Recently, in collaboration with this paper, Bahk and Shakouri have extensively modeled the prospects of reducing the thermal conductivity of PbTe through minority carrier blocking by heterjunctions [8]. In both cases, minority carrier blocking shows great promise for increasing zT through improving the Seebeck coefficient and reducing the thermal conductivity. In other examples of unique heterojunctions which can improve thermoelectric efficiency, Tynell et al. [9] have created a superlattice of conductive oxides (ZnO) and organic compounds (hydroquinone) and seen significant reductions in thermal conductivity [9].

Two-carrier temperature-dependent Seebeck coefficient

The Seebeck coefficient for a material with one type of carrier increases as the Fermi level moves towards the center of the semiconductor band gap. This occurs for semiconductors at high temperature or low doping as determined in the non-degenerate case by Eq. (1).

$$S_{n,p} = \pm \frac{k_B}{e}\left(r + \frac{5}{2} + \ln\frac{2(2\pi m_{n,p}^* k_B T)^{3/2}}{h^3 n,p}\right)(V/K) \qquad (1)$$

where $m_{n,p}^*$ is the effective mass of electrons or holes, r is the scattering parameter, k_B is the Boltzmann's constant, h is the Planck's constant, e is the charge on an electron, and n and p are the electron and hole concentrations. It is important to note that the Seebeck coefficient is negative for electrons and positive for holes, and can therefore go to zero or change sign when there is mixed n-type and p-type conduction. As shown in Eq. (2), the net Seebeck coefficient, S_T, is a combination of the negative Seebeck coefficient, S_n, and the positive Seebeck coefficient, S_p, weighted by the electron mobility, μ_n, electron concentration, hole mobility, μ_p, and hole concentration.

$$S_T = \frac{S_n\mu_n n + S_p\mu_p p}{\mu_n n + \mu_p p} \qquad (2)$$

As mentioned previously, when designing a thermoelectric material for use at high temperature, there have only been two options to overcome problems with intrinsic carrier activation: use a material with a wide band gap or increase the extrinsic doping. Wide band gap semiconductors are better at high temperature because the thermally activated intrinsic carrier density depends exponentially on the band gap energy. Higher extrinsic doping helps because it more heavily weights the majority carrier Seebeck coefficient, as demonstrated in Eq. (2). However, if you could add minority carrier blocking layers, and essentially reduce the mobility of the minority carrier, this would lighten the effect of the minority carrier Seebeck coefficient and improve the total Seebeck coefficient.

Figure 1a describes a typical n-type thermoelectric material, where the Fermi level is close to the conduction band edge and the temperature gradient has established an electron concentration gradient from the hot side to the cold side. Figure 1b shows the scenario where the same material is being used at higher temperatures, and thermally activated carriers are dominating the material's Seebeck coefficient. The Fermi level is positioned near the middle of the energy gap and electrons and holes are both present in appreciable concentrations. There is very little net charge difference between the hot and cold side. Figure 1c demonstrates the usefulness of a wide-band gap hole blocking region in an n-type thermoelectric. The holes cannot flow from the hot to the cold side and an appreciable net Seebeck coefficient is maintained. Figure 1d shows similar benefits for using a wide-band gap electron blocking region in a p-type thermoelectric.

AlSb/InAs sample design and predicted band structure

To test this concept, we have decided to use a simple material system. We use p-type InAs for the main semiconductor and p-type AlSb layers to modify the Seebeck coefficient. InAs and AlSb have been researched in depth by MBE before [10] because the semiconductors are closely lattice-matched and have very different band gap energies. As seen in Figure 2, the band gap of AlSb is ~1.55 eV and InAs is ~0.36 eV at 300 K.

The valence band offset between AlSb and InAs is only ~0.15 eV while the conduction band offset is ~1.35 eV. This combination of band offsets applies itself well to blocking the flow of electrons perpendicular to the heterojunction interface. InAs/AlSb is also a good model system because the "roll-over" in Seebeck coefficient should occur at relatively low
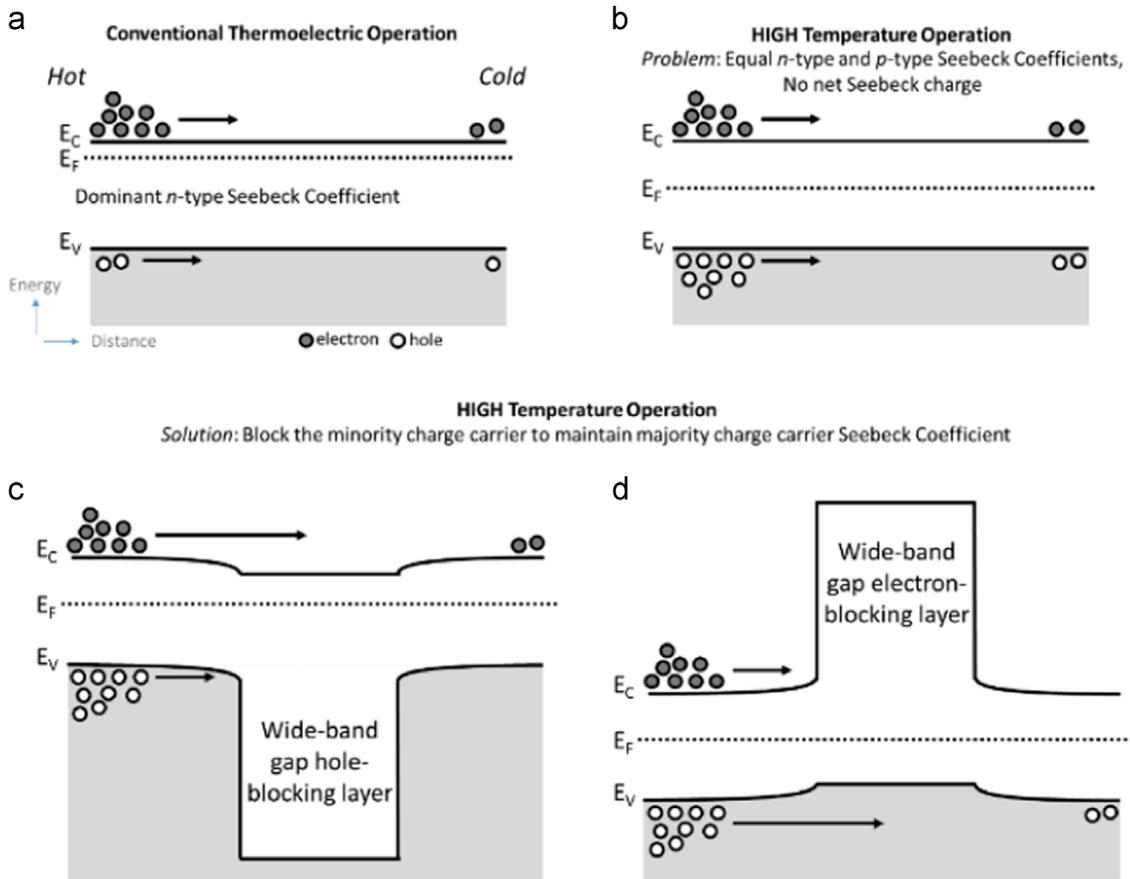
Figure 1 (a) Energy band diagram for a conventional thermoelectric material. (b) Energy band diagram for the same material operating at a much higher average temperature, where there is an appreciable concentration of minority carriers present due to thermal activation of electrons across the band gap. This scenario shows very low net charge difference between the hot side and cold side. (c) and (d) Energy band diagrams for hole-blocking and electron-blocking regions to enhance n-type and p-type thermoelectric materials, respectively.
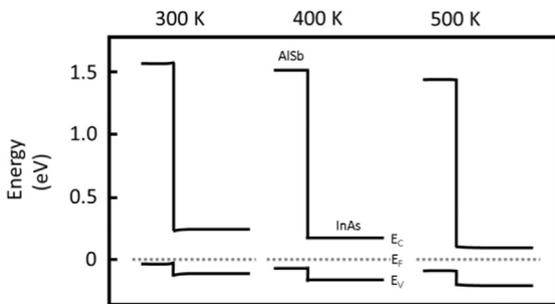

Figure 2 Calculated heterojunction between lightly p-doped InAs and heavily p-doped AlSb, at 300, 400, and 500 K. The Fermi level depends highly on temperature, especially for small band gap materials.

Figure 3 Band diagram for (a) p+InAs/p+AlSb/p+InAs/pInAs which should show enhanced Seebeck coefficient due to minority carrier blocking, and (b) p+InAs/pInAs, which should not show enhancement.

temperatures and difficult substrate removal and layer encapsulation [11] should not be necessary at the relevant measuring temperatures. The only disadvantage to using a small band gap semiconductor like InAs is the presence of a surface accumulation layer [12-15], which is caused by Fermi level surface pinning above the conduction band edge. This additional thin degenerate electron layer will be evident and noted in the measurement results.
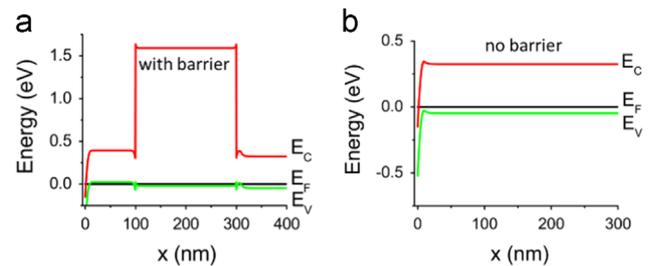
Sample fabrication

Two samples were grown by molecular beam epitaxy, each having the same sample structure, but different Be doping concentrations in the active layer. Ideally, AlSb electron blocking layers would be used throughout the entire composite, but for MBE grown samples, the transport properties of that superlattice would have to be measured cross-plane
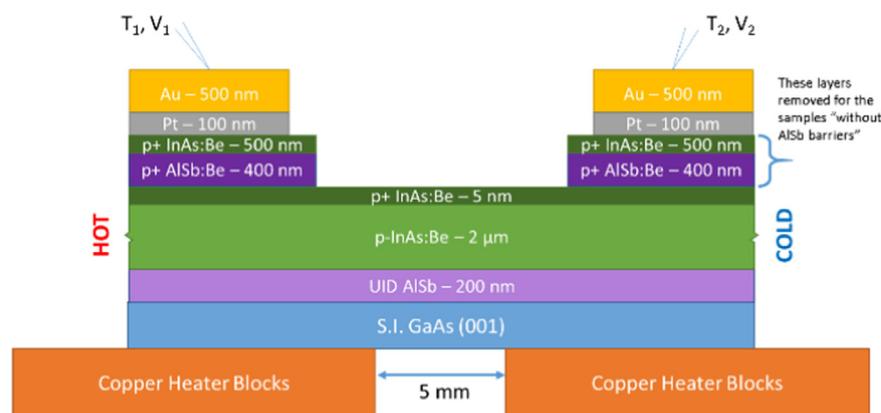
Figure 4 Cartoon schematic for the finished InAs sample with AlSb barrier layers, as it might be measured. Note that the layer thicknesses are not to scale relative to each other.

[16], which is inherently difficult for electrical conductivity and Seebeck coefficient. For this study, we used a simple structure, which could be measured in-plane. We grew a Be-doped 2 μm-thick InAs layer with a 300 nm-thick AlSb buffer on a (100) semi-insulating GaAs substrate. The GaAs substrate was used because it is cheaper and electrically insulating at room temperature. On top of the Be-doped InAs layer, we grew a thin 5 nm-thick heavily Be-doped InAs layer, a heavily Be-doped 500 nm-thick AlSb layer, and a heavily Be-doped 400 nm-thick InAs cap layer. The "heavy" doping in each of these thinner layers was $\sim 2 \times 10^{-19}$ cm^{-3}. The band diagram, calculated using a Poisson-Schrodinger solver, is shown in Figure 3.

To utilize the minority carrier barriers in the intended manner, the samples were processed so that the AlSb barriers were only at the metal contacts, with the main InAs layer measured in-plane between two heater blocks, as shown in Figure 4. The sample without AlSb barrier layers is exactly the same but without the top InAs or AlSb layer.

To make this structure, the MBE-grown films were fabricated with typical semiconductor processing tools. The metal stack (100 nm Pt, 500 nm Au) was defined lithographically and then deposited using an e-beam evaporator. Pt was used because of its fairly large work function, which aligns well with the InAs valence band edge, and because it is relatively stable to high temperatures. Then the metal contacts and a very thin perimeter were covered with photoresist, again using photolithography. The InAs exposed region between contacts was wet etched with a solution of $H_2O:H_2O_2:H_3PO_4$ (concentration: 15:5:1 by volume), which selectively etches InAs over AlSb. Then the AlSb newly exposed region was wet etched with a solution of $H_2O:H_2O_2:HCl$ (concentration: 100:1:100 by volume), which selectively etches AlSb over InAs.

The Seebeck coefficients were measured from a linear fit of voltage versus temperature difference [17] at each temperature data point, in vacuum, from 300 to 600 K. The electrical conductivity was measured using the 4-point probe method or the Van der Pauw method, also from 300 to 600 K. From 100-400 K, the commercially available thermal transport option (TTO) was used in a Quantum Design physical property measurement system (PPMS). At room temperature, Hall and Van der Pauw measurement were made to determine carrier density and mobility.

Measurement results

The temperature dependent Seebeck coefficient, electrical conductivity, and power factor are shown in Figure 5 for two pairs of samples. In Figure 5a, we show the results for the high Be doping sample ($\sim 3 \times 10^{18}$ Be atoms per cm^3), with and without AlSb barrier layers. The Seebeck coefficient and electrical conductivity for both samples is similar at 300 K, but from 350 to 500 K, the Seebeck coefficient is higher for the sample with the AlSb barrier layers, by up to 50 μV/K. This results in almost a 100% increase in power factor at 425 K, which is quite remarkable. In Figure 5b, we show the results for the low Be-doped sample ($\sim 1 \times 10^{18}$ Be atoms per cm^3), with and without AlSb barrier layers. For this Be doping, the Seebeck coefficient is almost 100 μV/K higher from 200 to 400 K. For this temperature range, the difference in electrical conductivity of the samples with and without AlSb barriers is minor. This results in an increase in power factor of 150 W/m K^2, an increase of 200%.

To better understand the effect of the AlSb electron blocking layers, we conducted Van der Pauw and Hall measurements, which are shown in Table 1. Again we note that the conductivities of the samples do not change dramatically with and without AlSb barriers. It is remarkable, yet not unexpected, that the Hall coefficient becomes more positive for both pairs of InAs samples, with and without barriers, suggesting that a higher hole concentration is being measured when AlSb barriers are present.

Analysis and discussion

The Seebeck coefficient and electrical conductivity were calculated in the manner described by Wagener et al. [18] accounting for the degenerate and non-degenerate regimes. These fits are shown in Figures.6 and 7 by the dotted red lines. The model was then adjusted to remove the effect of the n-type surface accumulation layer and to lower the number of thermally activated minority carriers. These results are represented by the black line in Figures 6 and 7. We use the input of acceptor concentrations and the ratio of electron mobility to hole mobility to fit our data, with good agreement. The increase in Seebeck coefficient is greater for the InAs samples with less Be doping, which intuitively makes sense. For
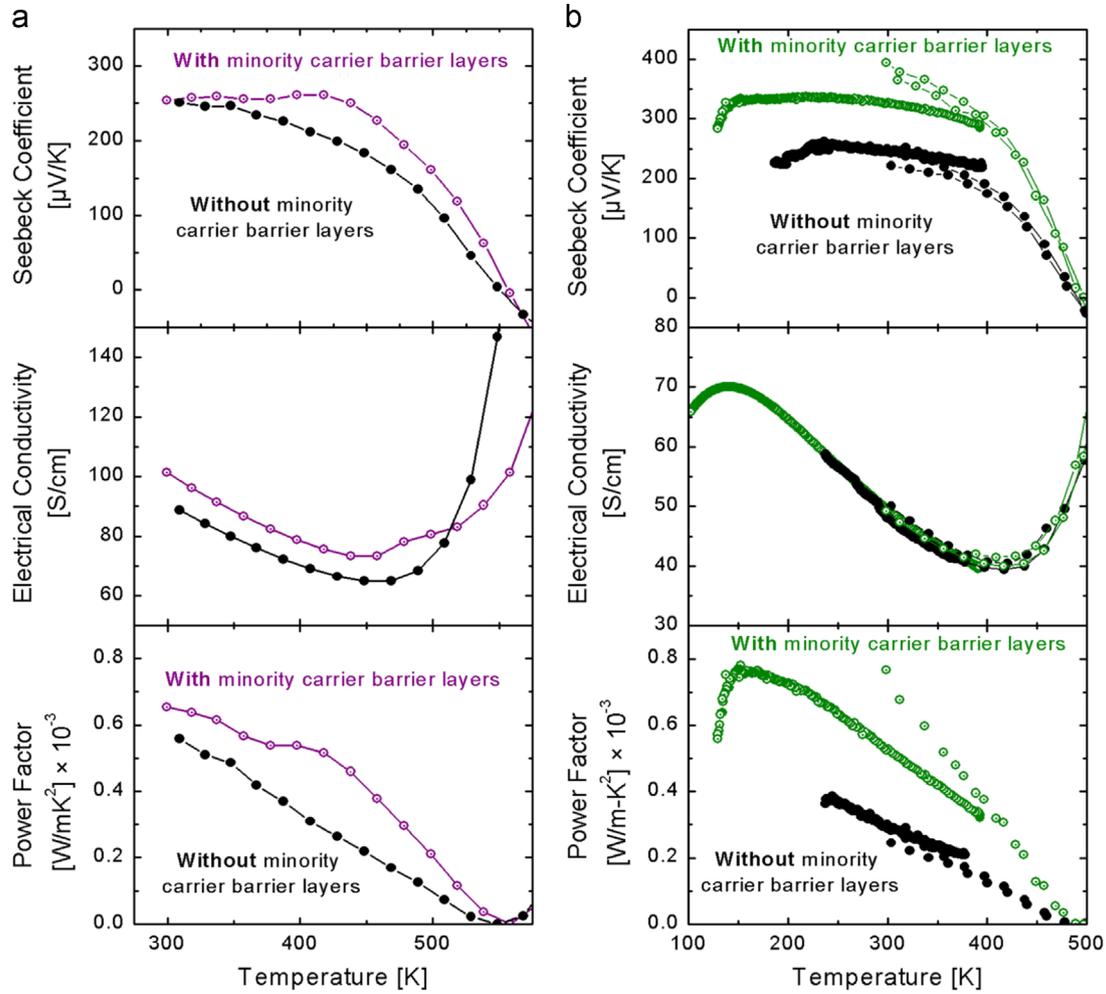
Figure 5 Measurement of increased Seebeck coefficient due to incorporation of minority carrier barriers. (a) InAs doped with $\sim 3 \times 10^{18}$ Be atoms/cm³, and (b) InAs doped with $\sim 1 \times 10^{18}$ Be atoms/cm³. In (b) the Seebeck data from 100 K to 400 K was measured using the thermal transport option on a Quantum Design PPMS, while the Seebeck data from 300 K to 500 K was measured under vacuum on a calibrated home-built system. Each measurement used a separate device fabricated from the same wafer.

Table 1 Room temperature carrier density and mobility of Be-doped InAs with and and without AlSb barriers.

		Electrical conductivity	Hall coefficient	Carrier density	Mobility
		(S/cm)	(cm³/C)	(cm⁻³)	(cm²/V-s)
High Be doping	With AlSb barrier	97.79	4.19×10^{-5}	7.45×10^{18}	82
	Without AlSb barrier	80.41	1.07×10^{-4}	2.90×10^{18}	172
Low Be doping	With AlSb barrier	49.4	-5.80×10^{-4}	-5.38×10^{17}	-573
	Without AlSb barrier	47.18	-1.23×10^{-5}	-2.54×10^{19}	-12

example, if the extrinsic doping is lower, the thermally activated minority carriers will be more detrimental. By removing their input on Seebeck coefficient, we see a bigger increase. This is a further proof that the increase in Seebeck coefficient is due to electron blocking in these samples.

Intuitively, blocking one type of carrier should lower the total electrical conductivity of the system, everything else being equal. Our calculations show us that this is true, but not to the extent we would expect. For instance, in Figure 8, we calculate that the electrical conductivity only changes by

~ 5 S/cm even when the minority carrier barrier is most pronounced. These calculations are under the same conditions to fit the high Be doped InAs Seebeck coefficient.

Conclusion

We have conceived and demonstrated an idea for improving Seebeck coefficient and power factor in semiconductor materials using careful band engineering. This solution
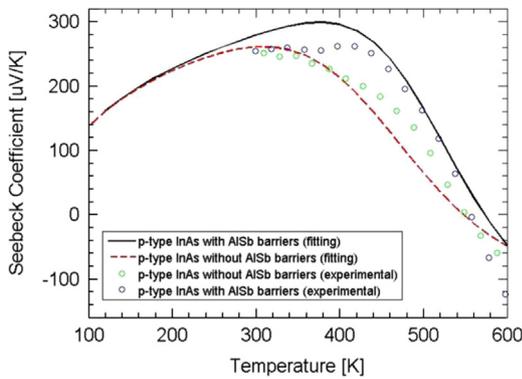
Figure 6 Fitted experimental data for highly Be-doped InAs. The dotted red line and green circles represent typical InAs, accounting for the surface accumulation layer. The black line and blue circles represent InAs with relatively fewer minority (holes) carriers and no surface accumulation layer contribution.
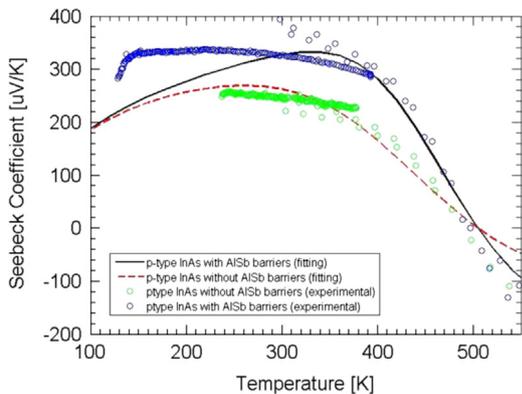

Figure 7 Fitted experimental data for low Be-doped InAs. The dotted red line and green circles represent typical InAs, accounting for the surface accumulation layer. The black line and blue circles represent InAs with relatively fewer minority (holes) carriers and no surface accumulation layer contribution.

addresses the problem of bipolar conductivity, which occurs in semiconductors at high temperature. When the concentration of thermally activated intrinsic carriers becomes appreciable, the Seebeck coefficient decreases and the thermal conductivity increases. We have shown that inserting wide band gap semiconductor layers in a narrow band gap semiconductor host can improve the Seebeck coefficient by blocking minority carriers. This idea increases the thermoelectric power factor by $2\times$–$2.5\times$ in our model system on p-type InAs with p+AlSb electron blocking layers. In addition, using a superlattice should lower the thermal conductivity [8]. In short, accounting for and managing the minority carrier transport should increase the thermoelectric figure of merit by simultaneously increasing the power factor and reducing thermal conductivity. The first steps to proving this concept have been demonstrated here.

Acknowledgments

The authors thank Je-Hyeong Bahk and Ali Shakouri, at the University of Purdue for helpful discussion on
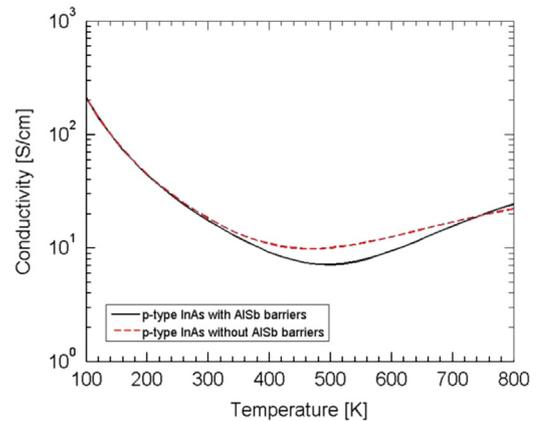

Figure 8 Theoretical electrical conductivity for p-type InAs, (a) accounting for the surface accumulation layer and intrinsic carriers (red dotted line) and (b) assuming no surface accumulation layer and fewer minority intrinsic carriers (black line). Of note is the relative similarity between both simulations.

References

[1] Stabler, F. R.,Commercialization of thermoelectric technology, In: Proceedings of the Material Research Soceity Symposium, Vol. 886, 0886-F01-04.1,Warrendale, PA; Materials Research Society; 1999, 2005).
[2] T. Kajikawa, J. Electron. Mater. 38 (2009) 1083–1088. http://dx.doi.org/10.1007/s11664-009-0831-2.
[3] J.O. Sofo, G.D. Mahan, Phys. Rev. B 49 (1994) 4565-4570.
[4] G.D. Mahan, J.O. Sofo, Proc. Natl. Acad. Sci. USA. 93 (1996) 7436.
[5] N. Gautam, H.S. Kim, M.N. Kutty, E. Plis, L.R. Dawson, S. Krishna, Appl. Phys. Lett. 96 (2010) 231107. http://dx.doi.org/10.1063/1.3446967.
[6] N. Gautam, S. Myers, A.V. Barve, B. Klein, E.P. Smith, D.R. Rhiger, L.R. Dawson, S. Krishna, Appl. Phys. Lett. 101 (2012) 021106. http://dx.doi.org/10.1063/1.4733660.
[7] S. Maimon, G.W. Wicks, Appl. Phys. Lett. 89 (2006) 151109. http://dx.doi.org/10.1063/1.2360235.
[8] J.H. Bahk, A. Shakouri, Appl. Phys. Lett. 105 (2014) 052106. http://dx.doi.org/10.1063/1.4892653.
[9] T. Tynell, A. Giri, J. Gaskins, P.E. Hopkins, P. Mele, K. Miyazaki, M. Karppinen, J. Mater. Chem. A 2 (2014) 12150–12152. http://dx.doi.org/10.1039/c4ta02381a.
[10] H. Kroemer, Phys. E Low-Dimens. Syst. Nanostruct. 20 (2004) 196-203. http://dx.doi.org/10.1016/j.physe.2003.08.003.
[11] J.-H. Bahk, G. Zeng, J.M.O. Zide, H. Lu, R. Singh, D. Liang, A.T. Ramu, P.G. Burke, Z. Bian, A.C. Gossard, A. Shakouri, J.E. Bowers, J. Electron. Mater. 39 (2010) 1125-1132. http://dx.doi.org/10.1007/s11664-010-1258-5.

[12] M. Noguchi, K. Hirakawa, T. Ikoma, Phys. Rev. Lett. 66 (1991) 2243–2246. http://dx.doi.org/10.1103/PhysRevLett.66.2243.

[13] L. Olsson, C. Andersson, M. Håkansson, J. Kanski, L. Ilver, U. Karlsson, Phys. Rev. Lett. 76 (1996) 3626–3629. http://dx.doi.org/10.1103/PhysRevLett.76.3626.

[14] D. Tsui, Phys. Rev. Lett. 24 (1970) 303–306. http://dx.doi.org/10.1103/PhysRevLett.24.303.

[15] L. Piper, T. Veal, M. Lowe, C. McConville, Phys. Rev. B 73 (2006) 195321. http://dx.doi.org/10.1103/PhysRevB.73.195321.

[16] G. Zeng, J.M.O. Zide, W. Kim, J.E. Bowers, A.C. Gossard, Z.X. Bian, Y. Zhang, A. Shakouri, S.L. Singer, A. Majumdar, J. Appl. Phys. 101 (2007) 034502. http://dx.doi.org/10.1063/1.2433751.

[17] J. De Boor, E. Müller, Rev. Sci. Instrum. 84 (2013) 065102. http://dx.doi.org/10.1063/1.4807697.

[18] M.C. Wagener, V. Wagener, J.R. Botha, Appl. Phys. Lett. 94 (2009) 262106, http://dx.doi.org/10.1063/1.3167822.

Peter Burke received his B.S degree from Lehigh University in Bethlehem, PA in 2008 and Ph.D. degree from University of California, Santa Barbara (UCSB) in Santa Barbara, CA in 2013, both in Materials Science. His work at UCSB focused on molecular beam epitaxy and processing of III-V semiconductor materials for thermoelectric applications.
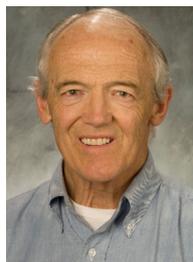
Benjamin Curtin received the M.S. degree from Iowa State University, Ames, Iowa, USA, and the Ph.D degree from University of California, Santa Barbara, California, USA, in 2009 and 2014, respectively.

He is currently a Failure Analysis Engineer at Aurrion, Inc. From 2009 to 2014, he was a graduate student at the University of California, Santa Barbara where he researched thermoelectric materials based on silicon nanowires. From 2008 to 2009, he was a graduate student at Iowa State University and researched photonic and plasmonic crystal back-reflectors in thin-film silicon photovoltaic devices.

John Bowers holds the Fred Kavli Chair in Nanotechnology, and is the Director of the Institute for Energy Efficiency and a Professor in the Departments of Electrical and Computer Engineering and Materials at UCSB. He is a cofounder of Aurrion, Aerius Photonics and Calient Networks. Dr. Bowers received his M.S. and Ph.D. degrees from Stanford University and worked for AT&T Bell Laboratories and Honeywell before joining UC Santa Barbara. Dr. Bowers is a member of the National Academy of Engineering and a fellow of the IEEE, OSA and the American Physical Society. He is a recipient of the OSA/IEEE Tyndall Award, the OSA Holonyak Prize, the IEEE LEOS William Streifer Award and the South Coast Business and Technology Entrepreneur of the Year Award. He and coworkers received the EE Times Annual Creativity in Electronics (ACE) Award for Most Promising Technology for the hybrid silicon laser in 2007.

Bowers' research is primarily in optoelectronics and photonic integrated circuits. He has published 10 book chapters, 600 journal papers, 900 conference papers and has received 54 patents. He has published 180 invited papers and conference papers, and given 16 plenary talks at conferences.

Arthur Gossard is professor of Materials and Electrical and Computer Engineering at University of California, Santa Barbara. His special interests are molecular beam epitaxy, the growth of quantum wells and superlattices and their applications to high performance electrical and optical devices. He is a fellow of the American Physical Society and the IEEE and a member of the National Academy of Engineering and the National Academy of Sciences.